

**NATURAL FREQUENCIES OF VIBRATION
OF SANDWICH PANELS**

by

MAGANBHAI PARBHUBHAI PATEL

B. Sc., University of Bombay, Bombay, India, 1949

B. S. University of Nebraska, 1952

B. S. University of Nebraska, 1953

A THESIS

submitted in partial fulfillment of the

requirements for the degree

MASTER OF SCIENCE

Department of Mechanical Engineering

**KANSAS STATE COLLEGE
OF AGRICULTURE AND APPLIED SCIENCE**

1959

LD
2668
T4
1959
P39
Spec. Collect,

TABLE OF CONTENTS

INTRODUCTION	1
THEORETICAL ANALYSIS	3
Core Equilibrium Equations	3
Strain Energy in the Cores	3
Strain Energy in the Face Due to Membrane Strains in the Facings. 8	
Strain Energy of the Facings Associated with the Bending of the Facings About Their Own Middle Surfaces.....	9
Total Elastic Strain Energy	10
Kinetic Energy of the Vibrating Strip	10
Frequency Criteria	11
OPERATION OF EQUIPMENT	11
EXPERIMENTAL PROCEDURE	15
COMMENTS ON THE PROCEDURE	19
PRESENTATION OF DATA AND SAMPLE CALCULATIONS.....	25
Presentation of Data	25
Sample Calculations	41
DISCUSSION OF TEST RESULTS	45
CONCLUSIONS	47
ACKNOWLEDGMENTS	48
NOMENCLATURE	49
REFERENCES	51
APPENDICES	52

INTRODUCTION

Sandwich construction consists of two relatively thin sheets of a material called facings, separated by and bonded to a relatively thick internal member called the core. The facings are usually made of material with high strength and stiffness whereas the core is usually a material of less density and comparatively low strength and stiffness. The resulting composite structure has an extremely high strength-weight ratio as compared with that obtainable through the use of a single homogeneous material. For this reason, it is widely used in construction of structural components in which weight is a major factor, such as guided missiles and air frames. Recently, improved techniques of bonding and fabrication are increasing its applications in many other industries such as the domestic appliance and marine, etc.

Prior to fabrication, the core is extremely flexible with seemingly little strength and the thin facings of the sandwich are incapable of resisting reasonable design loads in their own plane because of their elastic instability. However, once incorporated in a sandwich, the core becomes the structural center of a rigid panel which has strength and dimensional stability. Thus, the facings must be of a high strength material that will withstand outside fiber stresses; the core must withstand maximum shear which occurs at the center. The bonding agent -- adhesive, brazing, alloy or weld -- must transmit stresses from core to facing panels.

Although sandwich panels are rigid and strong, they are susceptible to damages from concentrated loads (panels used as floors in aircraft

have been damaged by the heels of ladies' high-heeled shoes). It is difficult to fasten panels with conventional rivets or screws unless the internal core is sufficiently strengthened in the area to be fastened. Vibration hazards to structures are well known. The study of vibration in sandwich panels which go into making guided missiles, aircraft frames, etc. is important. Because of its complex layered system, many variables have to be taken into account, a fact which makes the analysis of the problem more difficult. Much work of both theoretical and experimental nature has been done in the field of statics of sandwich structures, but, to the knowledge of the author, there is nothing in the literature to suggest that work in the dynamics field has been undertaken.

In view of these facts, Raville and Kimel (1) presented a mathematical derivation for calculating the natural frequencies of vibration of sandwich panels, simply supported on two opposite ends and constructed with isotropic facings and orthotropic cores.

The purpose of this thesis is to present an experimental verification of Raville and Kimel's theory, and to lay the groundwork for the development of vibration techniques for future investigations in this field at Kansas State College.

A series of vibration tests was performed on four sandwich panels, 120 in. by 6 in. in size, and of two different thicknesses (0.25 in. and 1.0 in.) supported knife edges. Data of resonating frequencies for various modes were obtained, and presented in tabular and graphical forms.

The natural frequencies of the same four beams, for free-free and clamped end conditions, were also obtained and included in this thesis.

The latter investigations were necessary to develop the experimental technique.

This thesis describes the outline of the theory and the test procedure used, and presents the results of the test.

THEORETICAL ANALYSIS

In their analysis, Raville and Kimel assumed that the core of the sandwich panel is capable of resisting only normal stresses perpendicular to the facings and shear stresses in planes perpendicular to the facings, which are treated by isotropic thin plate theory. It is also assumed that E_c , the transverse modulus of elasticity of core, is infinite.

The problem of the determination of natural frequencies of vibration associated with the cylindrical bending of a rectangular sandwich panel simply supported on two opposite edges and free on the other edges was analyzed. Modes of vibration corresponding to "face wrinkling" were not considered.

The dimensions of the sandwich panel strip and the co-ordinate system used in this analysis are shown in Fig. 1. Each facing is assumed to have the same physical properties.

Core Equilibrium Equations

A differential element of the deformed core is shown in Fig. 2. Summation of forces in the x and z directions, respectively, yields

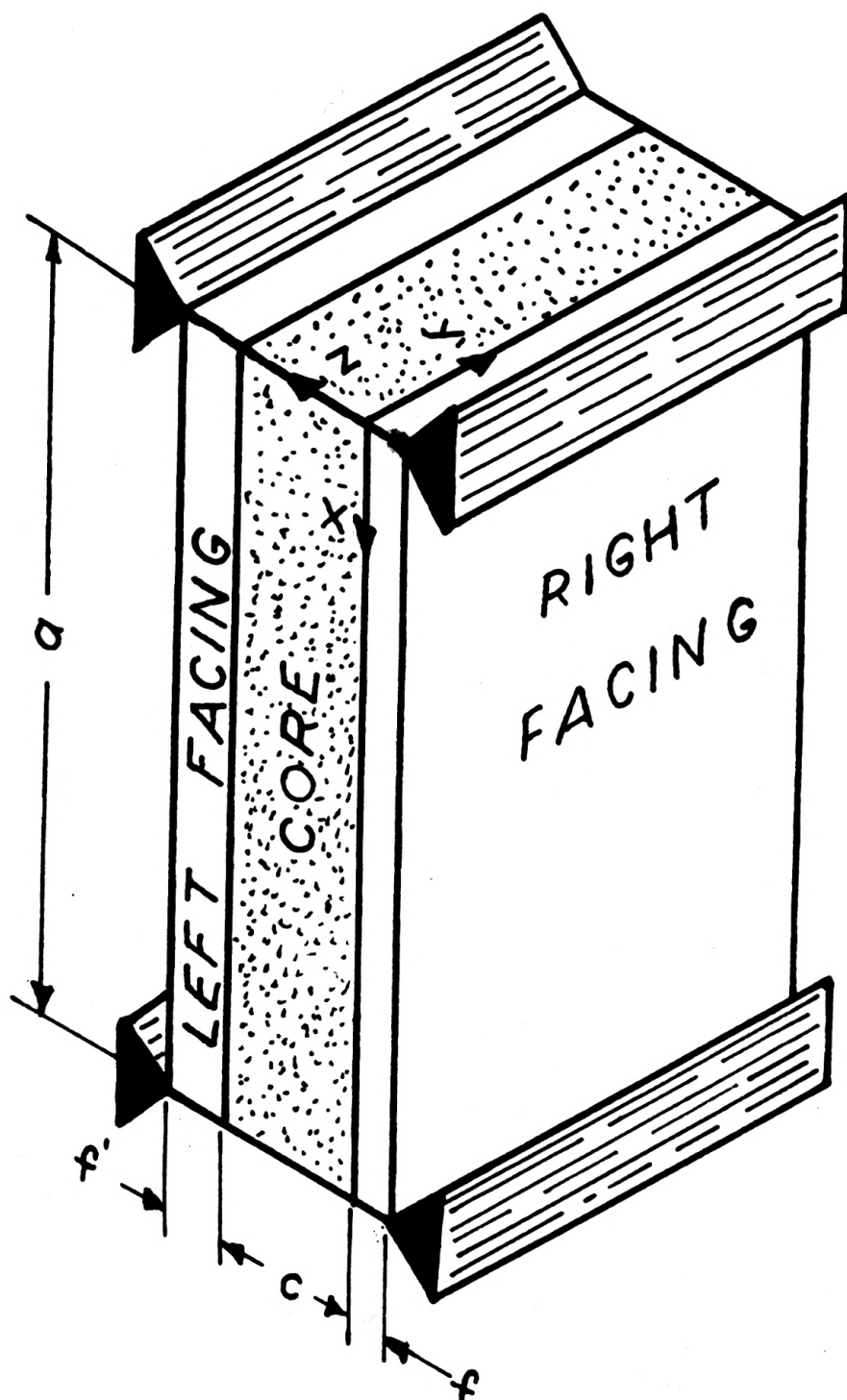


Fig. 1. Sandwich Strip

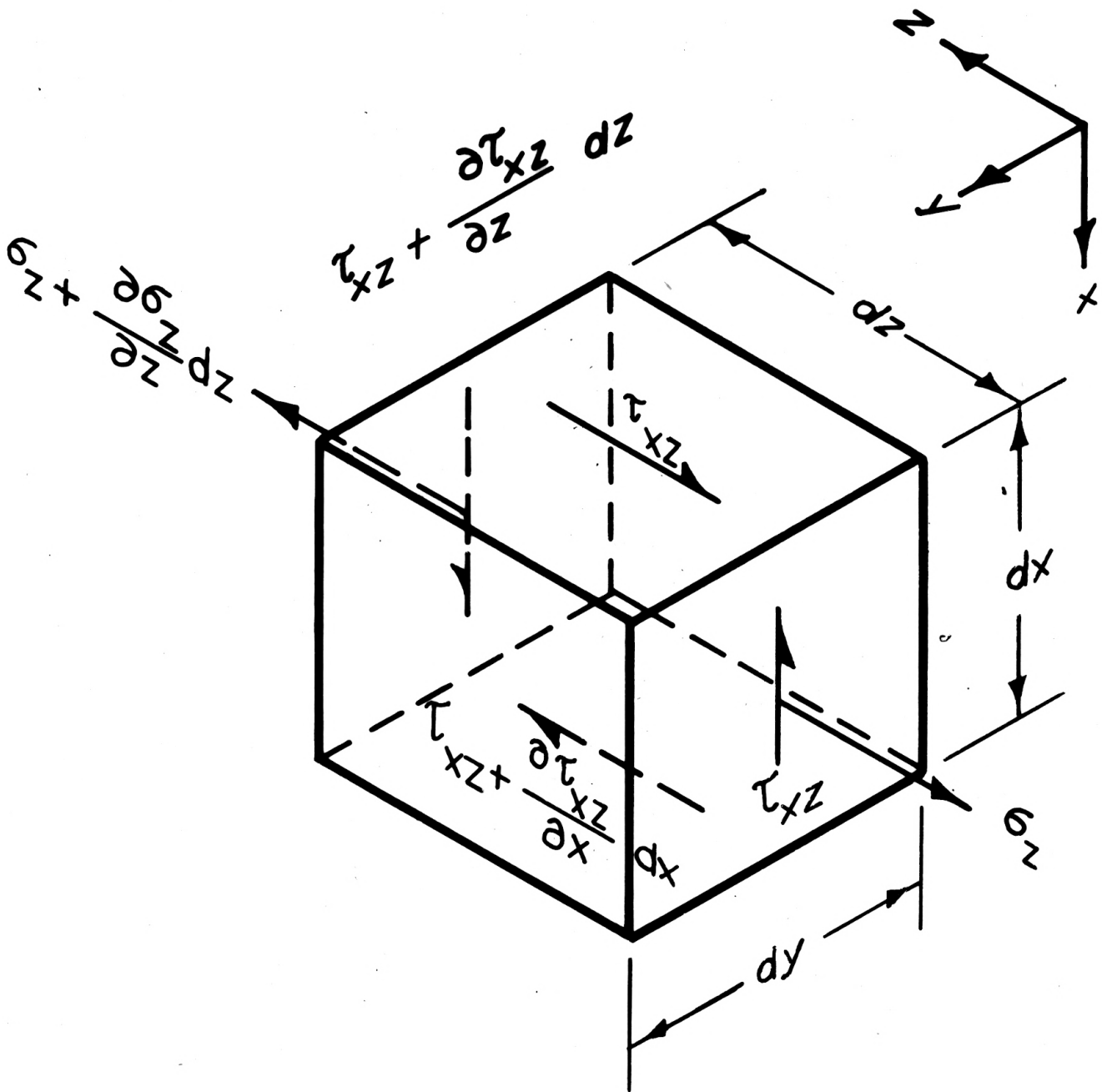


Fig. 2. Differential Element of the Core

the two equilibrium equations

$$\frac{\partial \tau_{xz}}{\partial z} = 0 \quad (1)$$

and

$$\frac{\partial \sigma_z}{\partial z} + \frac{\partial \tau_{xz}}{\partial x} = \delta \frac{\partial^2 w_c}{\partial t^2} \quad (2)$$

The boundary conditions are

$$w_c(0, a) \Big|_t = \frac{\partial^2 w_c}{\partial x^2}(0, a) \Big|_t = 0.$$

In order to satisfy the boundary conditions of the simply supported panel, as well as the core equilibrium equations, the core displacements are assumed to be of the forms

$$\tau_{xz} = \sum_{m=1}^{\infty} A_m \cos \frac{m\pi x}{a} \sin \omega_m t \quad (3)$$

and

$$w_c = \sum_{m=1}^{\infty} C_m \sin \frac{m\pi x}{a} \sin \omega_m t \quad (4)$$

where A_m and C_m are constants of integration.

Substituting (3) and (4) into (2) gives

$$\sigma_z = \sum_{m=1}^{\infty} \left[\left(\frac{m\pi}{a} A_m - \delta \omega_m^2 C_m \right) z + B_m \right] \sin \frac{m\pi x}{a} \sin \omega_m t \quad (5)$$

Substitution of (3) and (4) into the equation

$$\tau_{xz} = G_{xz} \left(\frac{\partial u_c}{\partial z} + \frac{\partial w_c}{\partial x} \right) \quad (6)$$

gives

$$u_c = \sum_{m=1}^{\infty} \left[\left(\frac{A_m}{G_{xz}} - \frac{m\pi}{a} C_m \right) z + F_m \right] \cos \frac{m\pi x}{a} \sin \omega_m t. \quad (7)$$

Equations (3), (4), (5) and (6) satisfy the core equilibrium equations (1) and (2), and the boundary conditions.

Strain Energy in the Cores

From (4) and (7), the core strains are expressed as

$$\epsilon_{zc} = \frac{\partial w_c}{\partial z} = 0 \quad (8)$$

$$\text{and } \gamma_{xzc} = \frac{\partial u_c}{\partial z} + \frac{\partial w_c}{\partial x} = \sum_{m=1}^{\infty} \frac{A_m}{G_{xz}} \cos \frac{m\pi x}{a} \sin \omega_m t. \quad (9)$$

The elastic strain energy of the core can be expressed as

$$V_c = \frac{1}{2} \int_0^a \int_0^c G_{xz} \gamma_{xzc}^2 dx dz. \quad (10)$$

Substituting (9) into (10) and integrating, gives

$$V_c = \frac{ac}{4G_{xz}} \sum_{m=1}^{\infty} A_m^2 \sin^2 \omega_m t. \quad (11)$$

Strain Energy in the Facings Due to Membrane Strains in the Facings

The membrane strains in the right and left facings, ϵ_{xM} and ϵ'_{xM} respectively, can be expressed in terms of the core displacements as follows:

$$\epsilon_{xM} = \left(\frac{\partial u_c}{\partial x} + \frac{f}{2} \frac{\partial^2 w_c}{\partial x^2} \right)_{z=0} \quad (12)$$

and

$$\epsilon'_{xM} = \left(\frac{\partial u_c}{\partial x} - \frac{f'}{2} \frac{\partial^2 w_c}{\partial x^2} \right)_{z=c}. \quad (13)$$

The elastic strain energy, V_{MF} , associated with the membrane strain in the right facing can be expressed as:

$$V_{MF} = \frac{E}{2(1-\nu^2)} \int_0^a \int_{-f}^0 \epsilon_{xM}^2 dx dz. \quad (14)$$

Substituting (12) into (14) and integrating gives

$$V_{MF} = \frac{Eaf}{4(1-\nu^2)} \sum_{m=1}^{\infty} \left(\frac{m\pi}{a} F_m + \frac{f}{2} \frac{m^2\pi^2}{a^2} C_m \right)^2 \sin^2 \omega_m t. \quad (15)$$

Similarly, for the left facing

$$V'_{MF} = \frac{Eaf'}{4(1-\nu^2)} \sum_{m=1}^{\infty} \left[-\frac{A_m}{G_{xz}} \frac{m\pi c}{a} \left(c + \frac{f'}{2} \right) C_m - \frac{m\pi}{a} F_m \right]^2 \sin^2 \omega_m t. \quad (16)$$

**Strain Energy of the Facings Associated with
the Bending of the Facings About
Their Own Middle Surfaces**

The bending strains, ϵ_{xB} and ϵ'_{xB} , in the right and left facings, respectively, can be expressed in terms of the core displacement as

$$\epsilon_{xB} = \left(z + \frac{f}{2}\right) \left(\frac{\partial^2 w_c}{\partial x^2}\right) \quad (17)$$

and

$$\epsilon'_{xB} = \left(z - c - \frac{f'}{2}\right) \left(\frac{\partial^2 w_c}{\partial x^2}\right). \quad (18)$$

From (17) and (4), the elastic strain energy V_{BF} , associated with strains due to bending of right facing about its middle surface, is

$$V_{BF} = \frac{E}{2(1-\nu^2)} \int_0^a \int_{-f}^0 \epsilon_{xB}^2 dx dz. \quad (19)$$

Therefore,

$$V_{BF} = \frac{E a f^3}{48(1-\nu^2)} \sum_{m=1}^{\infty} \frac{m^4 \pi^4}{a^4} C_m^2 \sin^2 \omega_m t. \quad (20)$$

Similarly, the elastic strain energy, V_{BF} of the left facing can be expressed as

$$V'_{BF} = \frac{E a (f')^3}{48(1-\nu^2)} \sum_{m=1}^{\infty} \frac{m^4 \pi^4}{a^4} C_m^2 \sin^2 \omega_m t. \quad (21)$$

Total Elastic Strain Energy

The total elastic strain energy, V , of the sandwich strip of unit width is

$$V = V_c + V_{MF} + V'_{MF} + V_{BF} + V'_{BF}. \quad (22)$$

Substituting equations (11), (15), (16), (20) and (21) into equation (22) gives

$$\begin{aligned} V = \sum_{m=1}^{\infty} & \left[\frac{a c}{4G_{xz}} A_m^2 + \frac{E a f}{4(1-\nu^2)} \left(\frac{m \pi}{a} F_m + \frac{f}{2} \frac{m^2 \pi^2}{a^2} C_m \right)^2 \right. \\ & + \frac{E a f'}{4(1-\nu^2)} \left[-\frac{A_m}{G_{xz}} \frac{m \pi c}{a} + \frac{m^2 \pi^2}{a^2} \left(c + \frac{f'}{2} \right) C_m - \frac{m \pi}{a} F_m \right]^2 \\ & \left. + \frac{E a [f^3 + (f')^3]}{48(1-\nu^2)} \frac{m^4 \pi^4}{a^4} C_m^2 \right] \sin^2 \omega_m t. \end{aligned} \quad (23)$$

Kinetic Energy of the Vibrating Strip

Kinetic energy T , of the vibrating strip is given by

$$T = \frac{1}{2} \rho \int_0^a \left(\frac{\partial w}{\partial t} \right)^2 dx \quad (24)$$

$$\text{Since, } w = w_c. \quad (25)$$

Equations (4) and (25) satisfy the boundary conditions

$$w(0, a) \Big|_t = \frac{\partial^2 w}{\partial x^2} (0, a) \Big|_t = 0$$

Therefore,

$$T = \frac{\rho \omega_m^2 a}{4} \sum_{m=1}^{\infty} C_m^2 \cos^2 \omega_m t. \quad (26)$$

Frequency Criteria

The vibration system is assumed to be conservative so that

$$\frac{\partial}{\partial A_m} (V_{\max} - T_{\max}) = 0, \quad (27)$$

$$\frac{\partial}{\partial C_m} (V_{\max} - T_{\max}) = 0, \quad (28)$$

and

$$\frac{\partial}{\partial F_m} (V_{\max} - T_{\max}) = 0. \quad (29)$$

Substituting maximum values of V and T from equations (23) and (26), leads to three linear, homogeneous equations in which A_m , C_m and F_m are unknown.

Such a system of equations can yield for A_m , C_m and F_m , solutions other than the trivial one in which $A_m = C_m = F_m = 0$, only if the determinant of these equations is equal to zero. This condition brings to the frequency equation from which the frequencies of the various modes of vibrations can be calculated. Thus, the resulting equation can be simplified to give

$$\omega_m^2 = \frac{m^4 \pi^4 E}{a^4 (1 - \nu^2) \rho} \left(\frac{I_T}{1 + m^2 s} + I_F \right). \quad (30)$$

OPERATION OF EQUIPMENT

A schematic diagram of the apparatus for a typical vibration test of a sandwich beam with free ends is shown on Plate I.

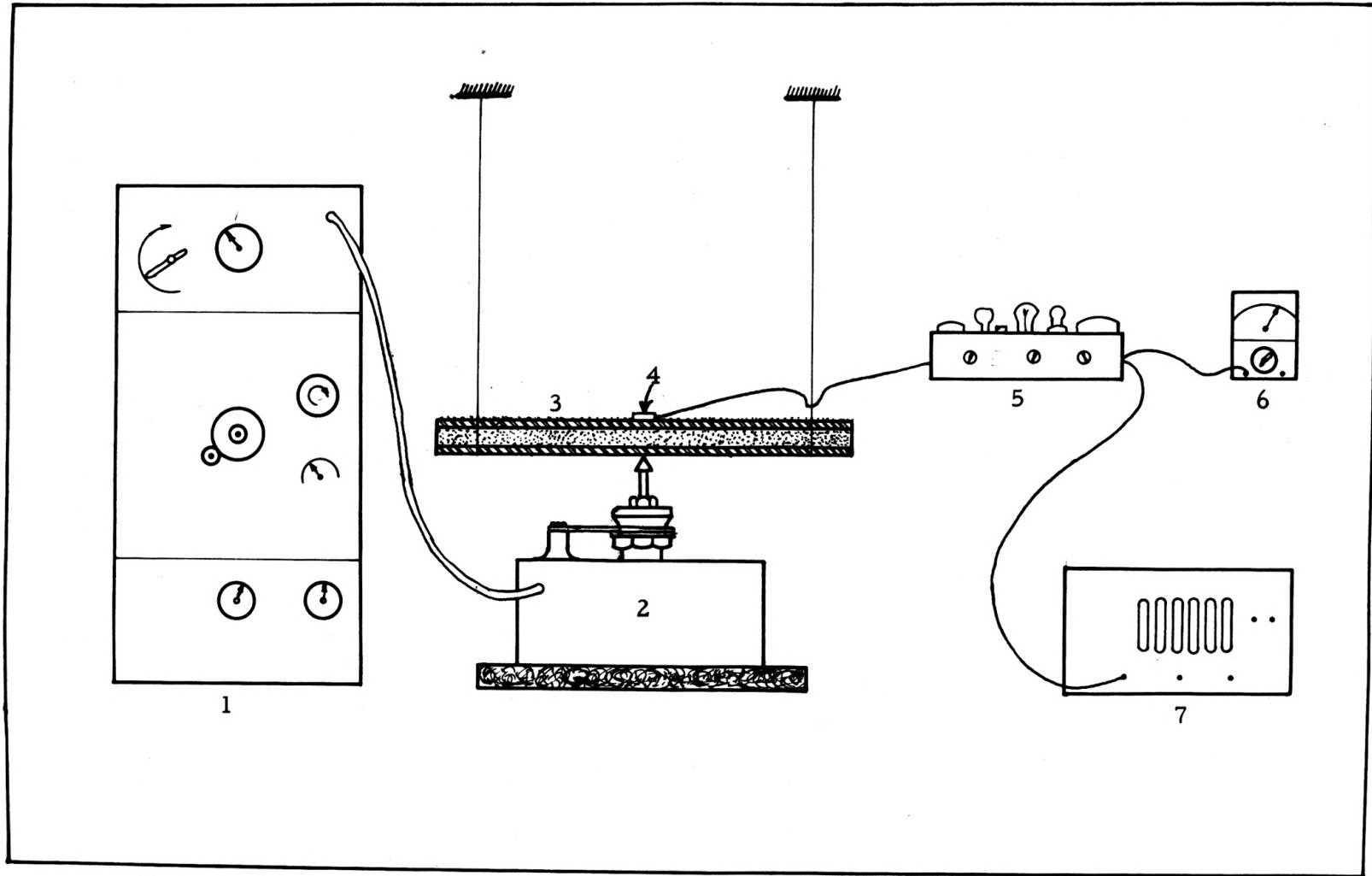
A sandwich beam is suspended by two strings s , at its nodal positions. The vibration exciter is placed under the beam at a position

EXPLANATION OF PLATE I

A Schematic Diagram of Experimental Equipment

Reference numbers:

- (1) Panel cabinet**
- (2) Vibration exciter**
- (3) Sandwich beam with sand Chladni figure**
- (4) Piezo electric pickup**
- (5) Amplifier**
- (6) Voltmeter**
- (7) Electronic frequency counter**



of maximum amplitude.

The Model C-31 vibration exciter by MB Manufacturing Company consists of a moving assembly including two flat spring flexures which support a threaded magnesium tube. Mounted on the tube are a driver coil and a signal generator coil, and a vibration pickup attachment table. The function of the vibration exciter is to generate a sinusoidal forcing function when the probe is properly matched to the specimen being vibrated. The driver coil which is supplied by a variable frequency alternating current, is suspended in a constant magnetic field. The amplitude and acceleration of the driver coil at a desired frequency are controlled by varying the applied current. The generated force depends upon the direct current in the field coil as well as the alternating current in the driver coil. The amplitude of the response depends not only on the generated force, but also on the dynamic properties of the system, including both the moving parts and the specimen. The motion of the force take-off (probe) is limited to plus or minus one-fourth-inch travel (giving a total excursion of one-half inch) or an acceleration of 100 g, whichever applies.

A piezo electric crystal pickup was used to measure the vibrations of the beams. It was held on the beam manually at lower frequencies to make it follow the beam in spite of its inertia. It was fixed by means of an adhesive tape at higher frequencies where the amplitudes are small.

The amplified signal of the pickup is lead simultaneously to a voltmeter and an electronic frequency counter.

The piezo electric effect is utilized in this crystal pickup to convert mechanical force (due to vibration) into electrical voltage. In other words, the voltage generated by the crystal is proportional to the force applied to it, and is therefore also proportional to the acceleration. The voltmeter gives a needle deflection proportional to the voltage generated by the crystal pickup.

The high speed electronic counter has an accurate crystal controlled timing gate. The unit automatically counts and displays in integer form any number of events which have occurred during a precise one-second counting interval. The events may be optical, physical or electrical occurrences translatable into voltage changes. The unit can also display the accumulated number of events during any integral number of seconds desired. If the timing gate is kept open for ten seconds, and the accumulated number of events divided by ten, the resulting figure for one second gives an accuracy of one decimal place.

EXPERIMENTAL PROCEDURE

The tests were carried out for the following end conditions:

1. Free-free,
2. Simply supported, and
3. Fixed-fixed.

In order to avoid complications due to end conditions, and to develop the technique of determining the natural frequencies of the beam, comparatively simple end conditions -- free ends -- were selected for the initial test.

Two symmetrical nodal positions and one antinodal position were calculated for each mode of vibration. These positions were carefully marked on the beam and used to support the beam and position the exciting probe, respectively. The beam was properly leveled to avoid any torsional effects while under transverse vibration test.

The vibration exciter with a rubber probe was placed under the specimen (Plate II) at the position of maximum amplitude.

After making proper electrical connections of the apparatus (see schematic diagram on Plate I), the following preliminary procedure was adopted for the proper operation of the Vibration Exciter;

1. The amplifier was turned on and allowed 10 to 15 minutes warm-up time.
2. The field supply was turned on and the field current was adjusted with the powerstat control to 0.7 amps. as specified by the manufacturer.
3. The desired range of operating frequencies was selected with the help of the decade range switch at the right-hand side of the oscillator panel.
4. The Amplitude Control, located just above the range switch on the oscillator panel was set at a 80 to 90 percent of the total rotation.

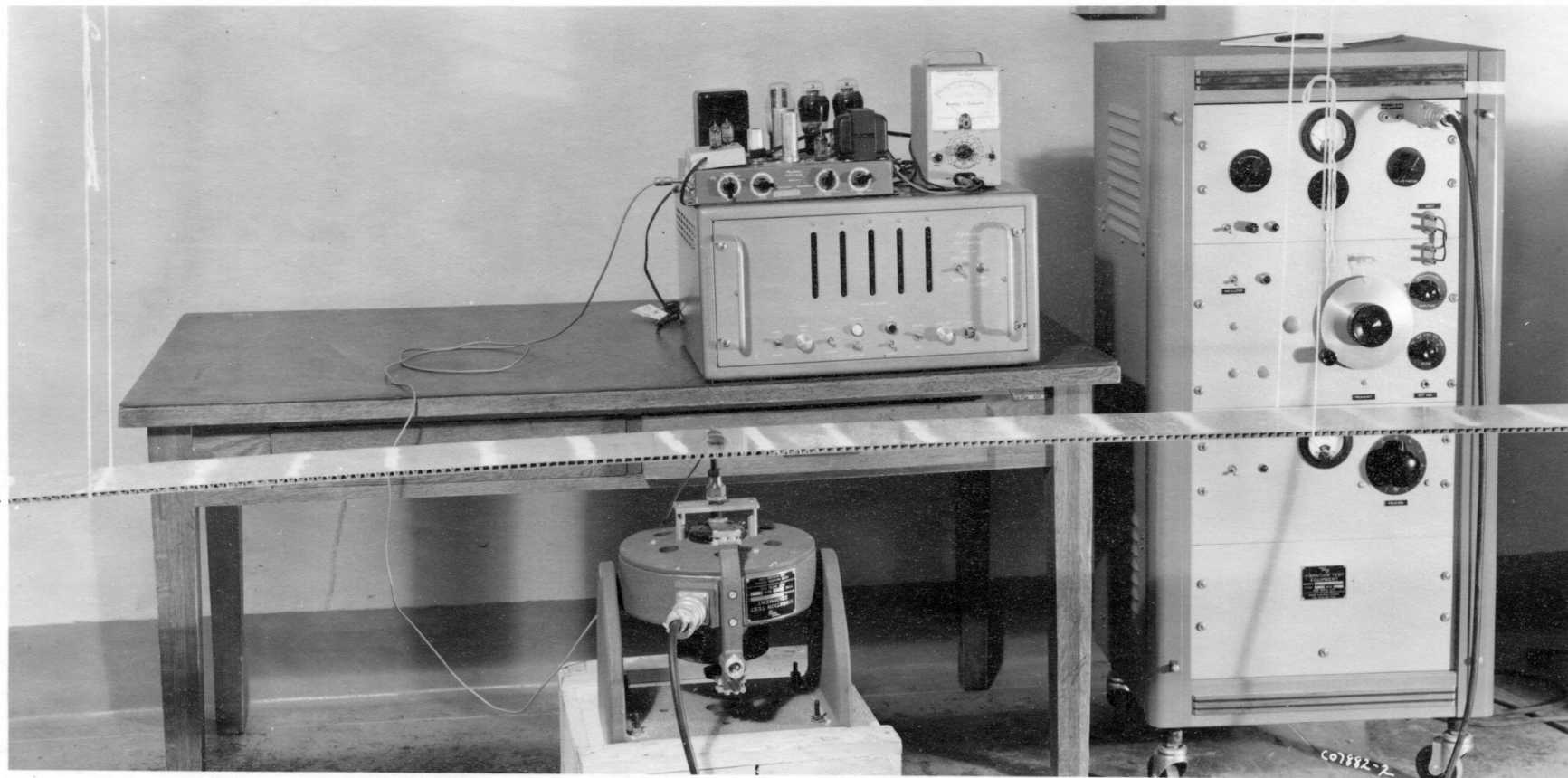
The desired input to the vibrator was established by adjusting the AC output control (top panel) and the amplitude control (middle panel). The frequency of vibration was controlled by the frequency dial on the oscillator panel.

The frequencies were slowly varied and when the forced frequency coincided with the natural frequency of the sandwich beam, resonance

EXPLANATION OF PLATE II

**Photograph of the vibration test setup
for free-free end conditions.**

Plate II



occurred. Resonance was detected by noticing a maximum voltmeter deflection, vigorous movement of sawdust or sand which was spread on the beam prior to the operation of the test, the formation of Chladni figures on the beam, and a peculiar change in the noise level (sound). The resonating frequency was read from the electronic counter panel. Sawdust collected at the nodal positions. The mode number in which the beam was resonating was determined by counting the nodal positions. The mode is one less than the number of nodes.

When the frequency was slightly altered, the Chladni pattern of sawdust was disturbed and the voltmeter deflection decreased. The next higher mode was excited by increasing the frequency until a new maximum voltmeter deflection was observed, and the Chladni figure corresponding to the higher frequency appeared.

The same technique for determining the natural frequencies of various modes was employed for the simply supported and clamped end conditions.

COMMENTS ON THE PROCEDURE

The symmetrical nodal positions were calculated before the operation of the test because if the beam is suspended at any other positions, the reactions cause couples at the supports, and the beam no longer has free-free end conditions. The positions of maximum amplitude (antinodes) are calculated and marked on the beam in order to determine where to place the vibration exciter. Both nodal and antinodal positions were calculated for various end conditions and are included in the Appendix.

The sawdust, being comparatively light and soft, moved with the beam at the lower frequencies and did not respond to the vibrations of the beam at higher frequencies. In order to get better Chladni patterns, fine Ottawa sand of uniform size was substituted for sawdust. The sand worked very satisfactorily and some of the patterns formed by it can be seen on Plate III.

Difficulties were encountered in exciting modes beyond the 15th because of the fact that the rubber probe, like a soft (low stiffness) spring, absorbed most of the vibration energy of the generated force of the exciter. These difficulties were solved by substituting plastic and steel probes with which it was possible to excite modes up to the 25th and 35th, respectively.

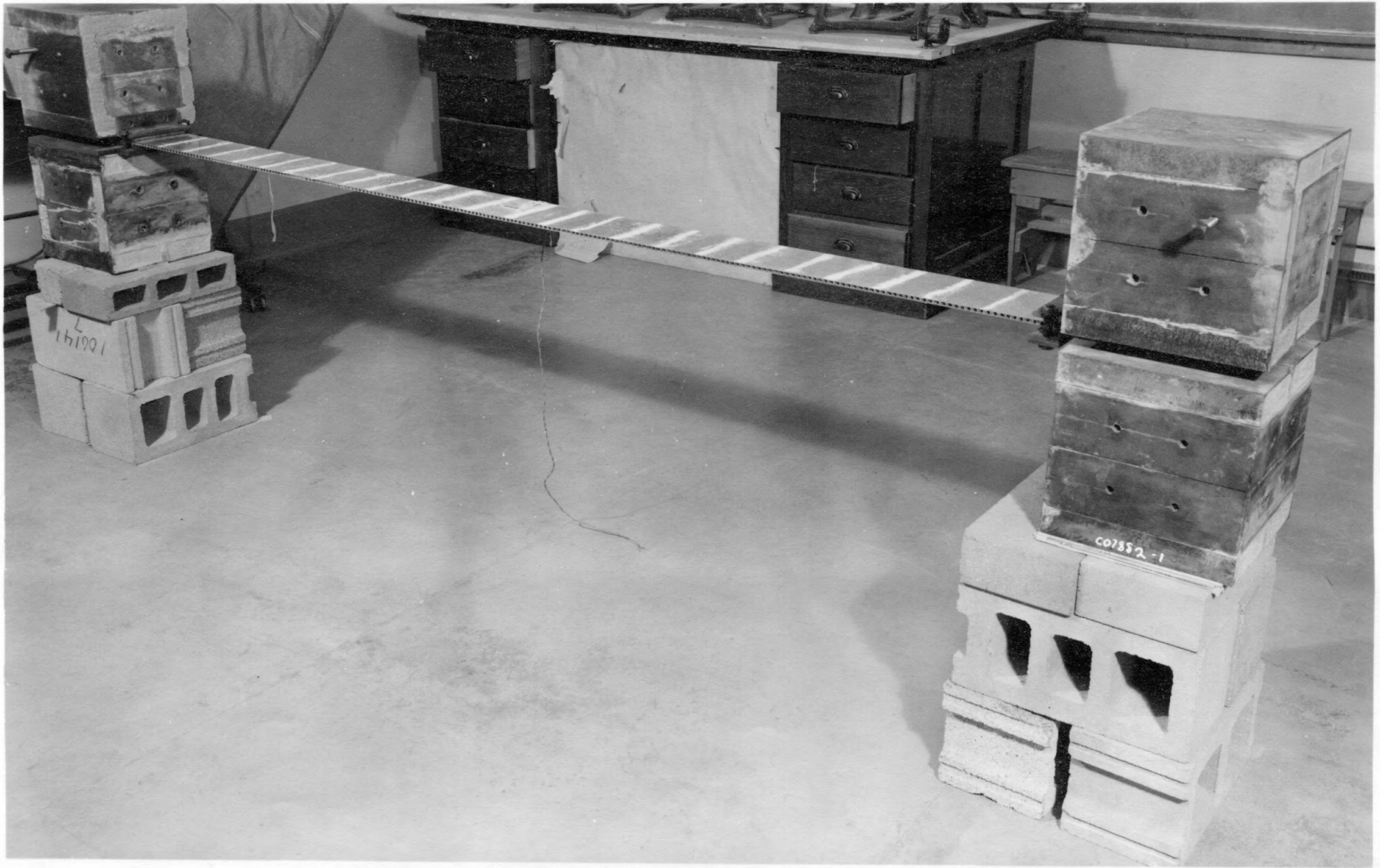
The performance of the probes of different materials can be explained by the electromechanical analogy as shown in Plate IV. The probe corresponds to a capacitance C . The natural frequencies of the system are given by $f_n = \frac{\alpha}{C}$, where α is a constant. If the capacitance is too high, only current with low frequencies can pass through the circuit, or, in other words, the circuit can be tuned for comparatively low frequencies only. The rubber probe corresponds to a relatively high capacitance, therefore, it could excite modes up to 15th only. Similar explanation can be offered for the behaviour of the plastic and steel probes.

Modes beyond 35th could not be excited because, at these modes, the Chladni patterns became smaller than the length between the two free edges and the beams began to vibrate as plates giving complex

EXPLANATION OF PLATE III

**Photograph of the vibration test setup
for clamped end conditions.**

Plate III



EXPLANATION OF PLATE IV

Electro-mechanical Analogy:



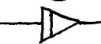

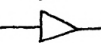

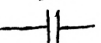
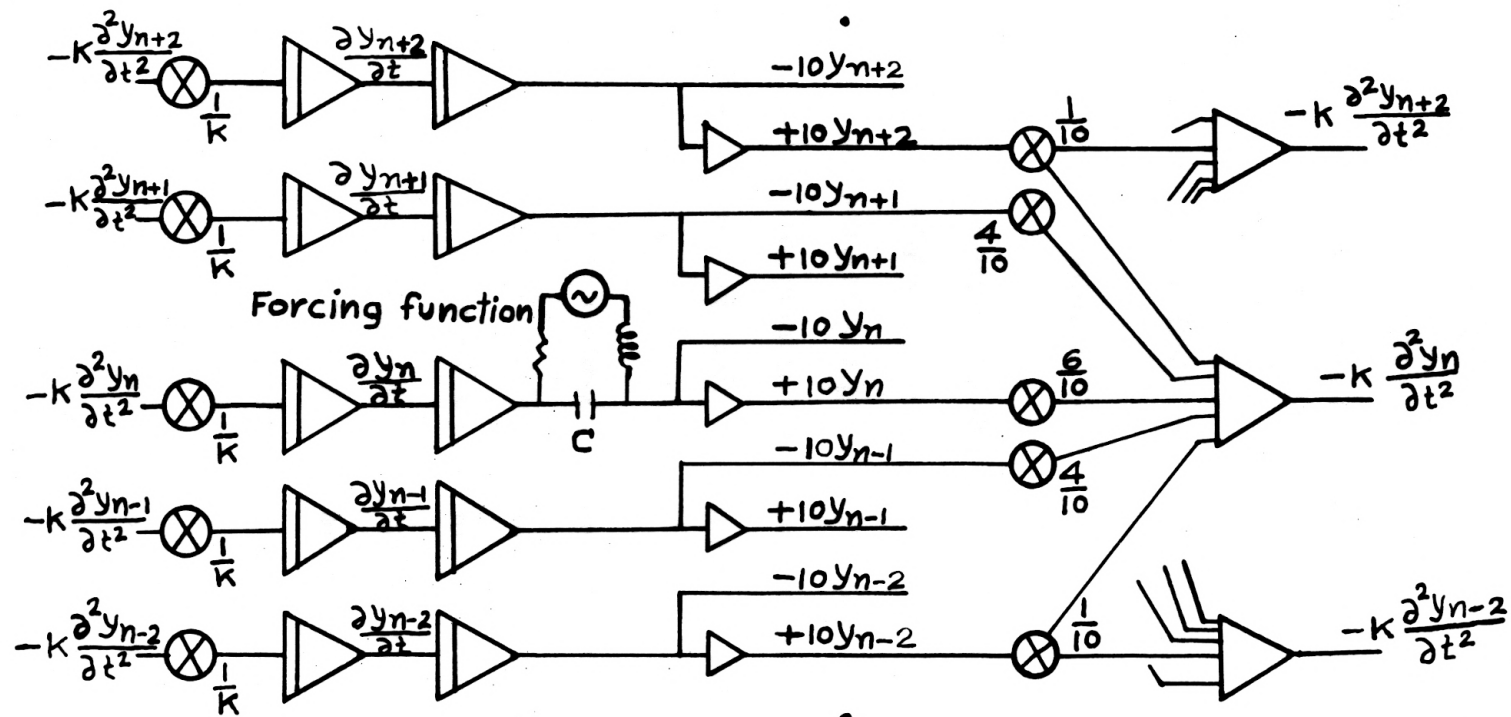
	Multiplier	Inductance	
	Integrator	Resistance	
	Summer	Source of power	
	Capacitance		

Plate IV



patterns not accounted for in the theory.

Another limiting factor was the force generating capacity of the vibration exciter; i.e., the acceleration at such frequencies was high, resulting in extremely small amplitudes to which the beam did not respond.

PRESENTATION OF DATA AND SAMPLE CALCULATIONS

Presentation of Data

Three different tests, corresponding to three different end conditions, were made on four samples of sandwich panels. Their physical dimensions and properties are given in Table 4.

The values of the natural frequencies which were determined experimentally for the different end conditions are recorded in Tables 1(a,b), 2(a,b), and 3(a,b).

Tables 1 (a,b) are for hinged or simply supported sandwich beams. A set of data for two beams (Nos. 2 and 5) of equal core thickness (0.25 in.) but of different core strength is presented in Table 1a. Beam No. 2 has a stronger core ($G_{xz} = 11,700$) than that of No. 5 ($G_{xz} = 4375$). Similarly, Table 1-b is for beams Nos. 10 and 7, of equal core thickness but of different strength. The facings are 0.016 in. thick in all the beams.

In all the cases, ω_e is the experimental value of the natural frequency. ω_m is obtained by solving the equation derived by Raville and Kimel (see sample calculations). ω_h is calculated by using the homogeneous beam theory (see sample calculations) with stiffness

Table 1-a. Frequencies of vibration of hinged beams Nos. 2 and 5.

No. of mode: m	Beam #2, $G_{xz} = 11,700$; Style 125-35; Type 20 (strong core)					Beam #5, $G_{xz} = 4375$; Style 60-20; Type 40 (weak core)				
	ω_e	ω_m	ω_h	ω_h/ω_e	% deviation of expt. freq.	ω_e	ω_m	ω_h	ω_h/ω_e	% deviation of expt. freq.
1	2	3	4	5	6	7	8	9	10	11
1	—	16.	2.571					2.624		
2	—		10.283					10.496		
3	—		23.137					23.616		
4	40		41.132					41.986		
5	61	65.613	64.269	1.0536	-7.562			65.602		
6	90		92.547	—		83		94.467	1.1382	
7	114		125.967	1.145				128.581		
8	178		164.528	—	7.94	158	158.0	167.943	1.0629	
9	201		208.231	1.170		239		212.552		
10	254	250.487	251.075	1.012	1.383	273	235.5	26.410		13.736
11	335		311.061	—		313		317.516	1.0144	
12	353	351.555	370.188	1.049	8.687	357	320.773	377.871	1.0585	10.147
13	423	406.908	434.457	1.025	3.963	396		443.473	1.1199	
14	479		503.867	1.052		445		514.324	1.156	
15	532	525.835	578.419	1.087	1.158	498	458.759	590.423	1.186	7.879
16	585		658.112	1.150		551		671.77		
17	644		742.946	1.1536		597		758.366		
18	712		832.923	1.1698		646		850.21	1.3161	
19	768	789.821	928.041	1.2084	-1.389	701		947.301	1.3514	
20	835		1028.300	1.2315	-3.071	754	702.10	1049.641	1.3921	6.883
21	897		1133.701	1.2639		810		1157.229	1.4287	
22	966		1244.243	1.2879		868		1270.06	1.4632	
23	1039		1359.926	1.3089		923		1388.15	1.5039	
24	1111		1480.751	1.333		971		1511.483	1.5566	
25	1172		1606.72	1.371	-4.81	1037	951.31	1640.064	1.5815	8.263
26	1251	1304.18	1737.827	1.389	-4.25	1093		1773.893	1.623	-10.93
27	1320		1874.077	1.4197		1151		1912.971	1.662	
28	1396		2015.47	1.4437		1198		2057.296	1.7173	
29	1470		2152.0	1.471		1268		2206.87	1.7404	
30	1536	1613.441	2313.675	1.51	-5.041	1317	1200.0	2361.692	1.7932	8.883
31	1613		2470.49	1.532		1376		2521.76	1.8327	
32	1691		2632.448	1.556		1431		2687.081	1.878	
33	1759		2799.55	1.5916		1490		2857.647	1.9179	
34	1833		2927.786	1.6213		1552		3033.462	1.955	
35	1919	2005.839	3149.169	1.641		1608		3214.525	1.999	

Table 1-b. Frequencies of vibration of hinged beams Nos. 10 and 7.

No. of mode: m	Beam #10, $G_{xz} = 9725$; Style 125-35; Type 20 (strong core)					Beam #7, $G_{xz} = 3500$; Style 60-20; Type 40 (weak core)				
	ω_e	ω_m	ω_h	ω_h/ω_e	% deviation of expt. freq.	ω_e	ω_m	ω_h	ω_h/ω_e	% deviation of expt. freq.
1	2	3	4	5	6	7	8	9	10	11
1			8.015					8.6724		
2			32.420					34.690		
3			72.420					78.052		
4	71		129.676	1.823		182		138.759	1.823	
5			202.619					216.811		
6	310	277.87	291.771		10.362			312.208		
7			397.133			359	355.16	424.950		1.069
8	435		518.705	1.1924	-6.0	445	433.621	555.036	1.1924	2.557
9	595		656.486	1.1033	5.529	578	513.124	702.467	1.1033	11.224
10	652		810.476	1.243				867.243	1.243	
11	758		980.676	1.294	-2.524	746		1049.364	1.2938	
12	865		1167.086	1.359		831	754.76	1248.830	1.359	9.174
13	957		1369.705	1.4312		927		1465.641	1.4312	
14	1062		1588.534	1.4958		1025		1699.80	1.4958	
15	1097		1823.572	1.6623	-11.94	1143	994.54	1951.297	1.6623	12.988
16	1223		2074.82			1211		2220.142	1.833	
17	1354		2342.276			1311		2506.33	1.912	
18	1464		2625.943	1.7936	-3.3196	1443	1231.0	2809.867	1.947	14.69
19	1579		2925.819	1.8529	-7.156			3130.75		
20	1677		3241.905	1.9331	-7.698	1639	1387.58	3468.973	2.1165	15.339
21	1794		3574.201	1.9923		1738	3824.542	3824.54	2.200	
22	-		3922.705			1817	4197.457	4197.457	2.3101	
23	1933		4287.42	2.2180		1895	4587.716	4587.716	2.4209	

Table 2-a. Frequencies of vibration of free-free beams Nos. 2 and 5.

No. of mode: m	Beam #2, $G_{xz} = 11,700$, $C = 0.25$ (strong core)			Beam #5, $G_{xz} = 4375$, $C = 0.25$ (weak core)		
	ω_e	ω_h	ω_h/ω_e	ω_e	ω_h	ω_h/ω_e
	expt.	homo.		expt.	homo.	
1					5.947	
2					16.397	
3					32.137	
4					53.125	
5	74.0	77.75	1.0506		79.359	
6	104.0	108.59	1.0441		110.841	
7	142.0	144.57	1.0181		147.569	
8	174.0	185.69	1.0672	189	189.544	
9	218.7	231.95	1.0606		236.77	
10	260.0	283.35	1.0898		289.235	
11	339.9	319.2	1.0648	333	346.951	1.0419
12	386.6	401.58	1.0388		409.914	
13	423.5	468.40	1.1060	438	478.124	1.1493
14	489.6	540.37	1.1104		551.581	
15	545.0	617.47	1.1330	524	630.284	1.2028
16	592.0	699.71	1.1820	564	714.234	1.266
17	661.8	787.10	1.1893	614	803.432	1.3085
18	732.4	879.62	1.2010	669	897.876	1.342
19	793.0	977.29	1.2324	722	997.567	1.3817
20	860.3	1080.09	1.2555	780	1102.506	1.4135
21	930.5	1188.03	1.277	834	1212.69	1.4541
22	1062.0	1301.12	1.2252	-	1328.12	-
23	1066.8	1419.34	1.3305	952	1448.80	1.5219
24	1138.5	1542.71	1.3550	-	1574.73	-
25	1211.7	1671.22	1.3792	1065	1705.90	1.602
26	1277.0	1804.86	1.4134	1121	1842.32	1.6435
27	1366.0	1943.65	1.4228	1174	1983.98	1.6899
28	1435.0	2087.57	1.4547	-	2130.89	-
29	1505.0	2236.63	1.4861	1292	2283.06	1.7671
30	-	2390.85	-	-	2440.47	-
31	1646.0	2550.19	-	1401	2603.12	1.858
32	1718.0	2714.68	-	-	2771.02	-
33	1791.0	2884.31	-	1504	2944.17	-
34	1864.0	3059.1	-	-	3122.56	-
35	1913.0	3238.98	-	1625	3306.21	-

Table 2-b. Frequencies of vibration of free-free
beams Nos. 10 and 7.

No. of mode: m	Beam #10, $G_{xz} = 9425$; $C = 1.0$ (strong core)			Beam #7, $G_{xz} = 3500$; $C = 1.00$ (weak core)		
	ω_e expt.	ω_h homo.	ω_h/ω_e	ω_e expt.	ω_h homo.	ω_h/ω_e
5	413	455.78	1.	242	262.153	1.0833
6				316	366.32	1.1592
7	413	455.78	1.1036	420	487.706	1.1368
8	513	585.424	1.1411	512	626.4315	1.2235
9	595	731.273	1.229	617	782.475	1.2681
10	693	893.326	1.2891	695	955.903	1.3754
11	808	1071.587	1.3262	789	1146.65	1.4533
12	890	1266.05	1.4225	880	1354.74	1.5395
13	1006	1476.73	1.4679	982	1580.166	1.6091
14	1107.0	1703.60	1.5389	1082	1822.94	1.6848
15	1239.6	1946.68	1.5704	1192	2083.05	1.7475
16	1306	2205.97	1.6891			
17	-	2481.46				
18	-					

Table 3-a. Frequencies of vibration of clamped beams Nos. 2 and 5.

No. of mode m	Beam No. 2; $G_{xz} = 11,700$; (strong core)					Beam No. 5; $G_{xz} = 4375$; (weak core)				
	ω_e experimental			ω_h		ω_e experimental			ω_h	
	Rubber	Plastic	Steel	Homo.beam	ω_h/ω_e	Rubber	Plastic	Steel	Homo.beam	ω_h/ω_e
1				9.10					9.29	
2				25.10					25.62	
3				49.19					50.21	
4				81.32		95			83.01	
5	116			121.48		120			123.99	1.033
6				169.67			168		173.19	
7	215	203		225.89	1.051	1.113	204		230.58	1.031
8				290.14					296.16	
9	315			362.43	1.151		304	347	369.95	1.217
10	387			442.74	1.144		364		451.93	1.066
11	448	473		531.09	1.186	1.123	422	443	542.11	1.285
12	517	544		627.47	1.214	1.153	481	506	640.49	1.224
13	590	608		731.88	1.241	1.204	545	569	747.07	1.332
14	666	688		844.32	1.268	1.227	610	631	861.84	1.371
15	759	762		964.79	1.295	1.266	679	697	984.82	1.413
16		837		1093.30	1.306			757	1115.99	
17	918	922		1229.84	1.340	1.334	826		1255.36	1.474
18		1004		1374.41		1.369	903		1402.93	1.52
19		1090		1527.01		1.401	969		1558.70	1.554
20		1175		1687.64		1.436	1035		1722.66	1.610
21		1263		1856.30		1.470		1111	1894.83	
22		1351		2033.00		1.505		1176	2075.19	1.706
23		1442		2217.73		1.538		1249	2263.75	1.765
24		1526		2410.48		1.580		1317	2460.51	1.812
25		1616		2611.27		1.616		1378		1.868
26		1710		2820.1		1.649		1455	2878.62	1.934
27		1793		3036.95		1.694		1520	3099.98	1.978
28		1882		3261.83		1.733		1597	3329.53	2.039
29		1966		3494.74		1.778		1657	3567.28	2.085
30				3535.00				1748	3813.23	2.153
31		2149		3984.68		1.854		1782	4067.37	2.182
32								1875	4329.73	2.282
33								1926	4600.26	2.310
34									4879.00	2.389
35								2125	5165.95	2.431

Table 3-b. Frequencies of vibration of clamped beams Nos. 10 and 7.

No. of mode m	Beam No. 10; $G_{xz} = 9725$; (strong core)							Beam No. 7; $G_{xz} = 3500$; (weak core)						
	ω_e experimental			ω_h	ω_h/ω_e			ω_e experimental			ω_h	ω_h/ω_e		
	Rubber	Plastic	Steel		Rubber	Plastic	Steel	Rubber	Plastic	Steel		Rubber	Plastic	Steel
3	131			155.09	1.134			141			165.95	1.177		
4	218			256.38	1.176			248	233		274.33	1.106	1.18	
5	321	375		382.98	1.193	1.021		325			409.81	1.261		
6		419		534.91		1.277		422			572.37	1.356		
7	526	555		712.16	1.36	1.283		554	547		762.04	1.375	1.40	
8	642			914.73	1.425				660		978.79		1.48	
9	765	784		1142.62	1.494	1.457			760		1222.64		1.61	
10		891		1395.82		1.566			865		1493.59		1.73	
11	1027	1047		1674.36	1.63	1.599			976		1791.63		1.84	
12		1146		1978.21		1.726			1095	1106	2116.76		1.93	
13		1290		2307.39		1.789			1205		2468.99		2.05	
14		1452		2661.88		1.833				1331	2848.30		2.14	
15		1570		3041.70		1.937				1414	3254.70			2.302
16			1667	3446.84			2.067			1591	3668.20			2.318
17			1836	3877.29			2.112			1692	4148.86			2.450
18			1941	4333.1			2.232			1835	4636.57			2.530
19			2030	4814.18			2.371			1942	5151.37			2.653

Table 4. Dimensions and physical properties of test beams.

Beam No.	Stiffness determined by static bending test EI lb-in. ²	Face thickness f in.	Core thickness c in.	Supplied by mfg. G _{xz}	Determined by vibration test G _{xz}	Total wt. of panel lb.	Style and Type
2	36,475	.016	0.25	11,700	11,540	3.040	125-35; 20
5	35,906	.016	0.25	4,375	6,630	2.875	60-20; 40
7	434,760	.016	1.00	3,500	6,870	3.185	60-20; 40
10	511,990	.016	1.00	9,725	9,220	4.300	125-35; 20

Modulus of Elasticity of aluminum facings, $E = 10.3 \times 10^6$ psi.
Poisson's Ratio = 0.33
Length of the sandwich panel = 120 in.
Width of the sandwich panel = 6 in.

determined experimentally using static bending tests.

Tables 2(a,b) and 3(a,b) are for free and clamped end conditions, respectively. For these two conditions, there are no values for theoretical, natural frequencies available.

The ratios $(\frac{\omega_h}{\omega_e})^2$ and $(\frac{\omega_h}{\omega_m})^2$ are calculated and

$$\left[\left(\frac{\omega_h}{\omega_e} \right)^2 - 1 \right] \text{ and } \left[\left(\frac{\omega_h}{\omega_m} \right)^2 - 1 \right] \text{ are plotted against the number}$$

of modes on log log graph paper. This representation was selected for the following reasons:

1. It exhibits the properties of the Raviile-Kimel theory.
2. Graphical representation is a good way to detect scattering and trends in the observed data.

According to the theory, the natural frequencies of the simply supported sandwich beam are given by the following equation:

$$\omega_m^2 = \frac{m^4 \pi^4 E}{a^4 (1 - \nu^2) \rho} \left(\frac{I_T}{1 + m^2 s} + I_F \right) \quad (a)$$

where,

$$s = \frac{\pi^2 c f f'}{a^2 (f + f')} \cdot \frac{E}{G_{xz} (1 - \nu^2)} \quad (b)$$

Those of equivalent homogeneous beams are given by,

$$\omega_h^2 = \frac{m^4 \pi^4 E_h I_h}{a^4 \rho} \quad (c)$$

where, I_h = moment of inertia of the cross-section of equivalent homogeneous beam,

and E_h = modulus of elasticity of the equivalent homogeneous beam.

The parameter s in (a) represents the effect of shear in the core of the sandwich. If s is set to zero, equations (a) and (c) become identical. Therefore, taking the ratio of (c) to (a) and considering

$$E_h = \frac{E}{(1 - \nu^2)}, \text{ gives}$$

$$\omega_m^2 = \frac{\omega_h^2}{I_h} \left(\frac{I_T}{1 + m^2 s} + I_F \right). \quad (d)$$

since, $I_h \sim I_T$ and $I_F \ll I_h$ for usual panels,

$$\omega_m^2 \cong \frac{\omega_h^2}{1 + m^2 s}. \quad (e)$$

Taking the logarithm of both sides and simplifying, gives

$$\log \left[\left(\frac{\omega_h}{\omega_m} \right)^2 - 1 \right] = 2 \log m + \log s. \quad (f)$$

(f) is the equation of a straight line ($y = mx + c$) on log log graph paper with a slope 2, and an intercept $\log s$.

If the experimental values ω_e are to verify the theory, they should satisfy equation (f). Therefore, the theoretical and observed values of natural frequencies were substituted in equation (f) and the results plotted on log log graph paper (Fig. 3 (a, b)).

As no theory exists for free-free and clamped beams, only the experimental data is presented in Figs. 4(a, b) and 5(a, b).

Columns 5 and 10 in Tables 1(a, b) for hinged beams show the percentage deviation of experimental values of natural frequencies from

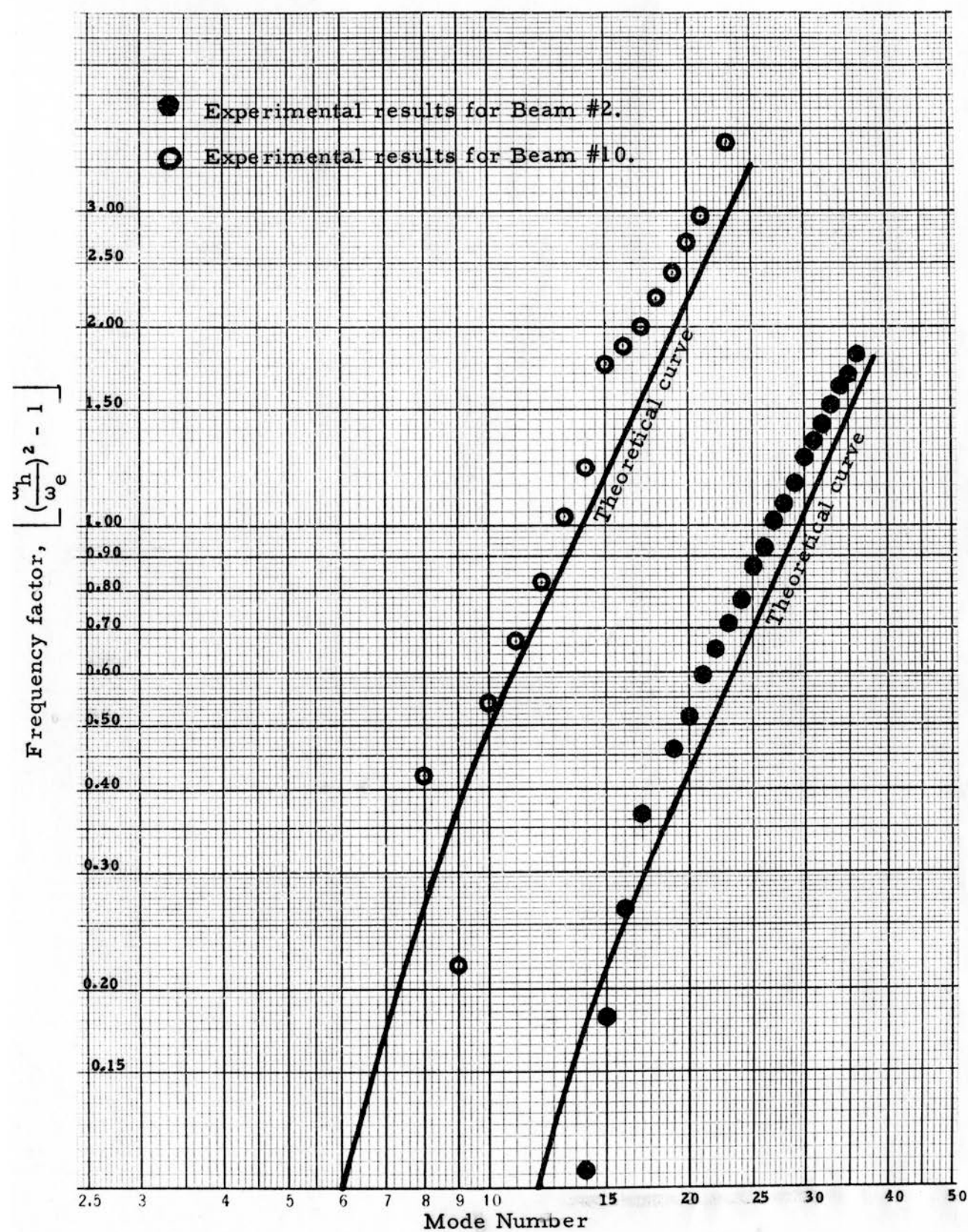


Fig. 3a. Theoretical curves and experimental results of hinged beams Nos. 2 and 10.

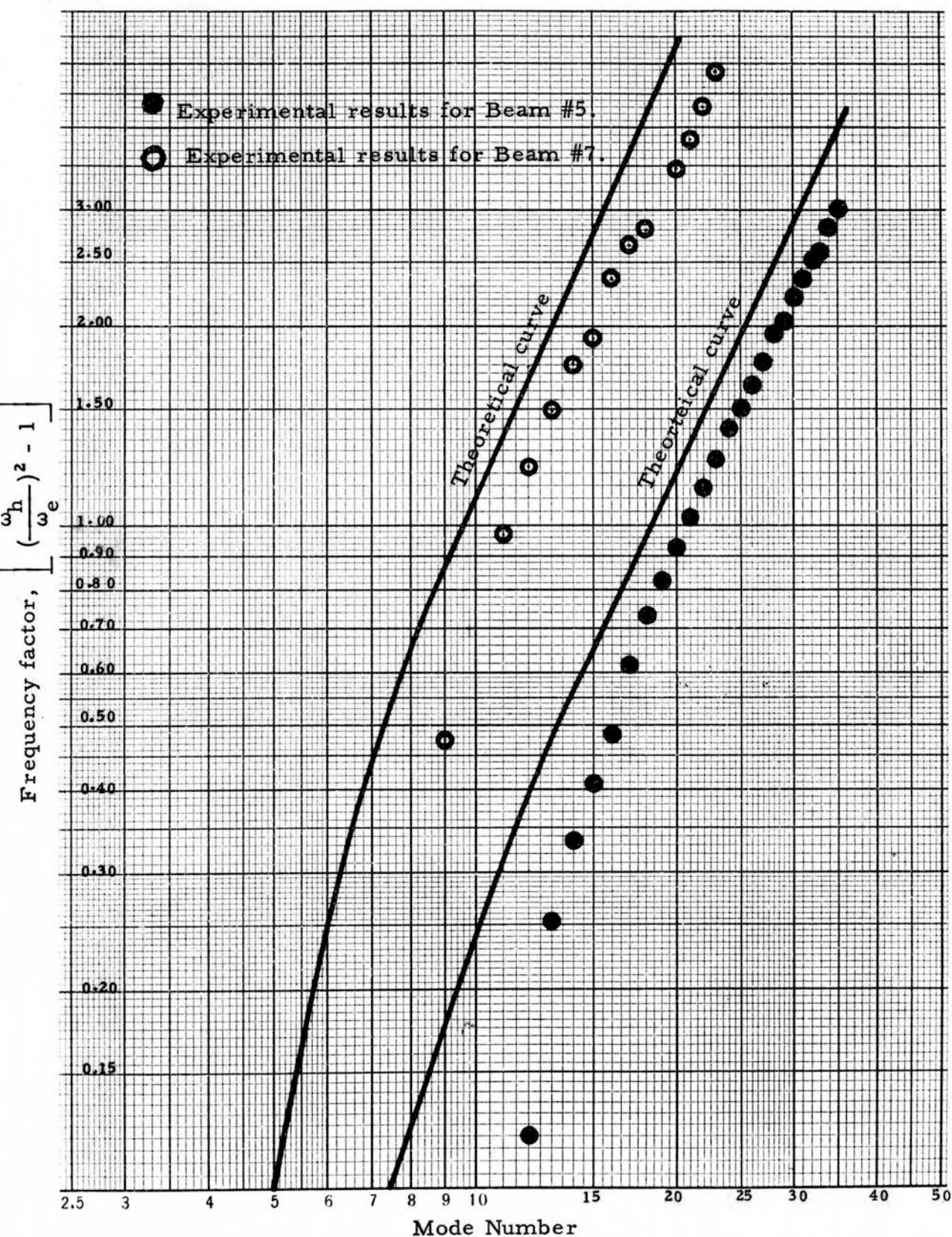


Fig. 3b. Theoretical curves and experimental results of hinged beams Nos. 5 and 7.

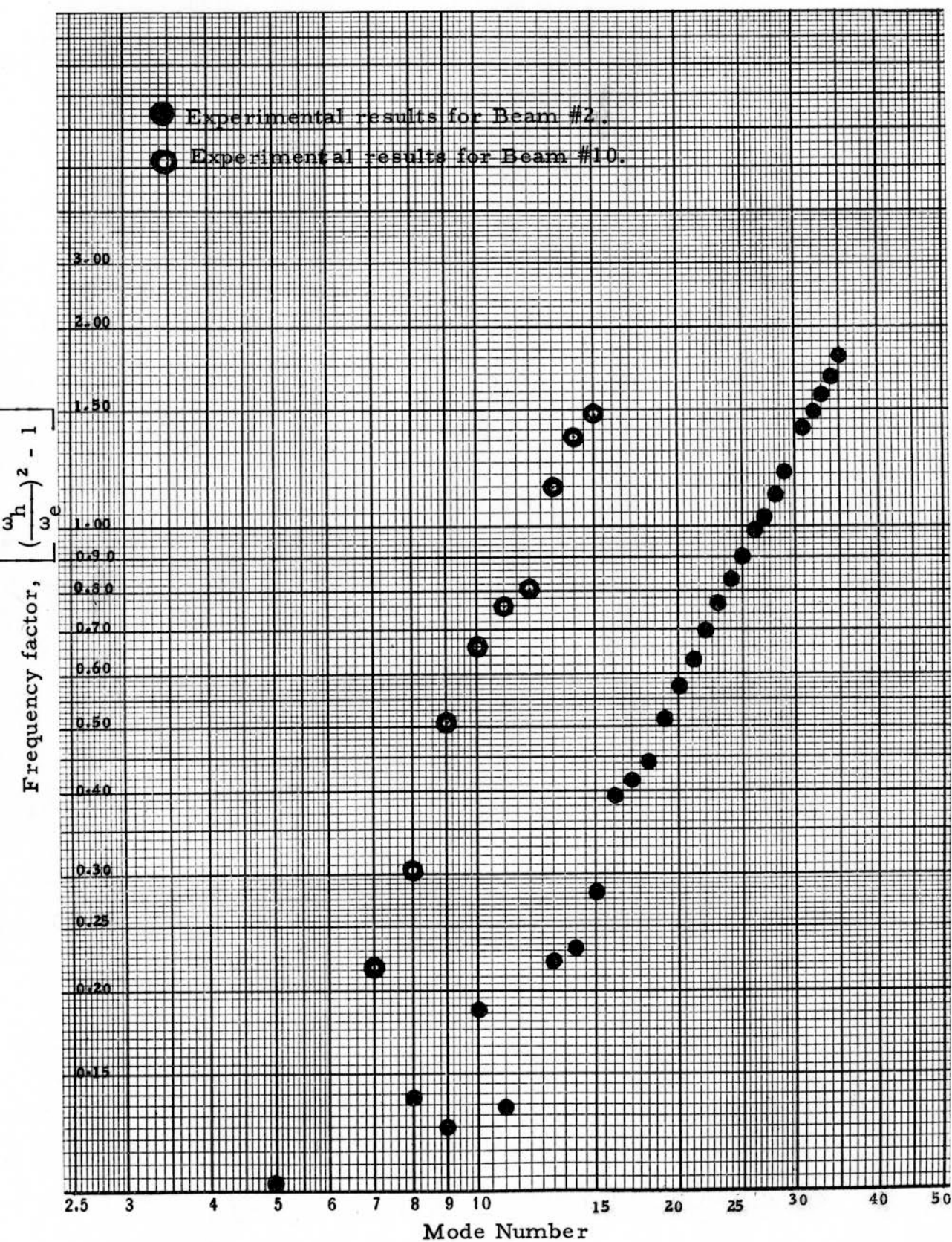


Fig. 4a. Experimental results of free-free beams Nos. 2 and 10.

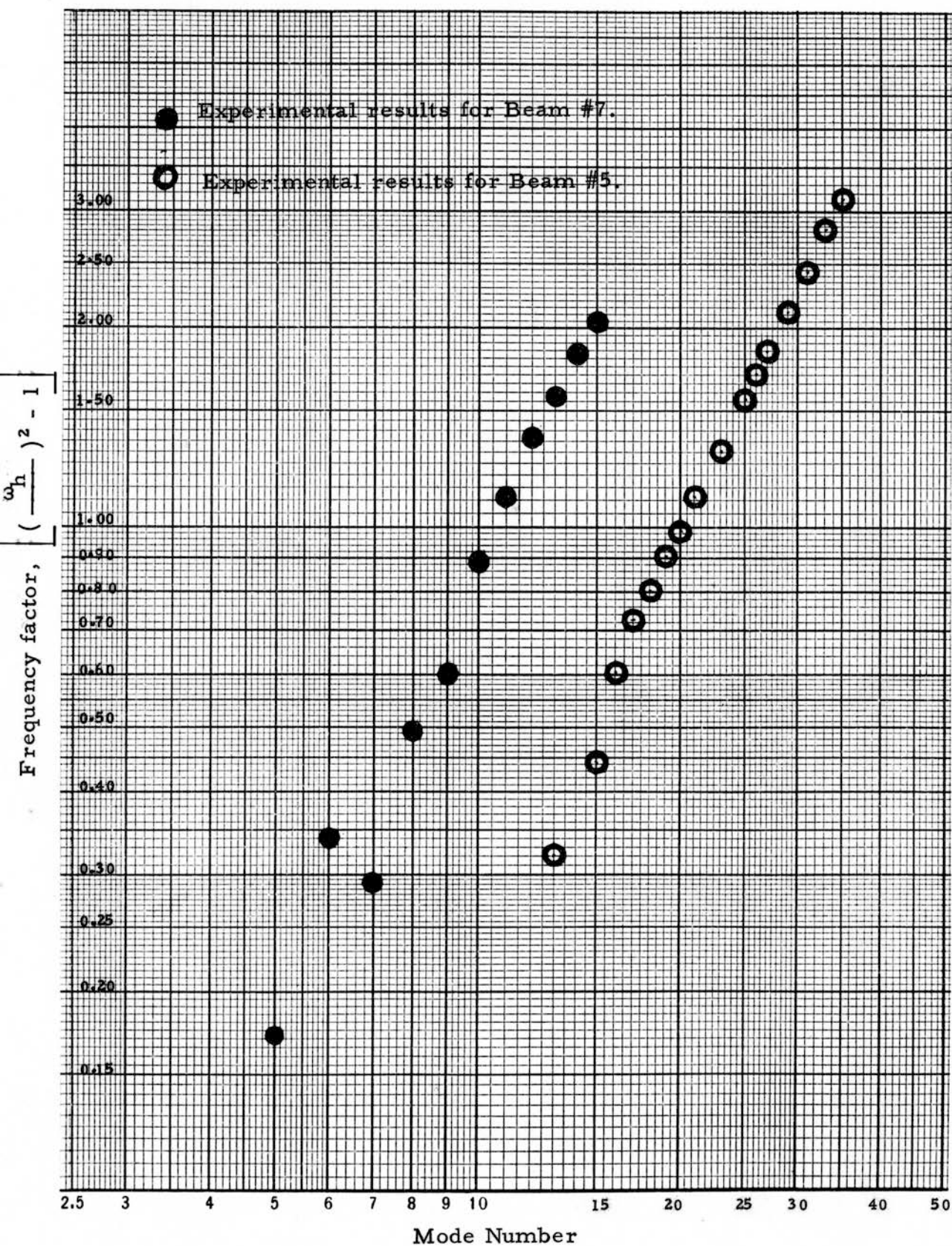


Fig. 4b. Experimental results of free-free beams Nos. 5 and 7.

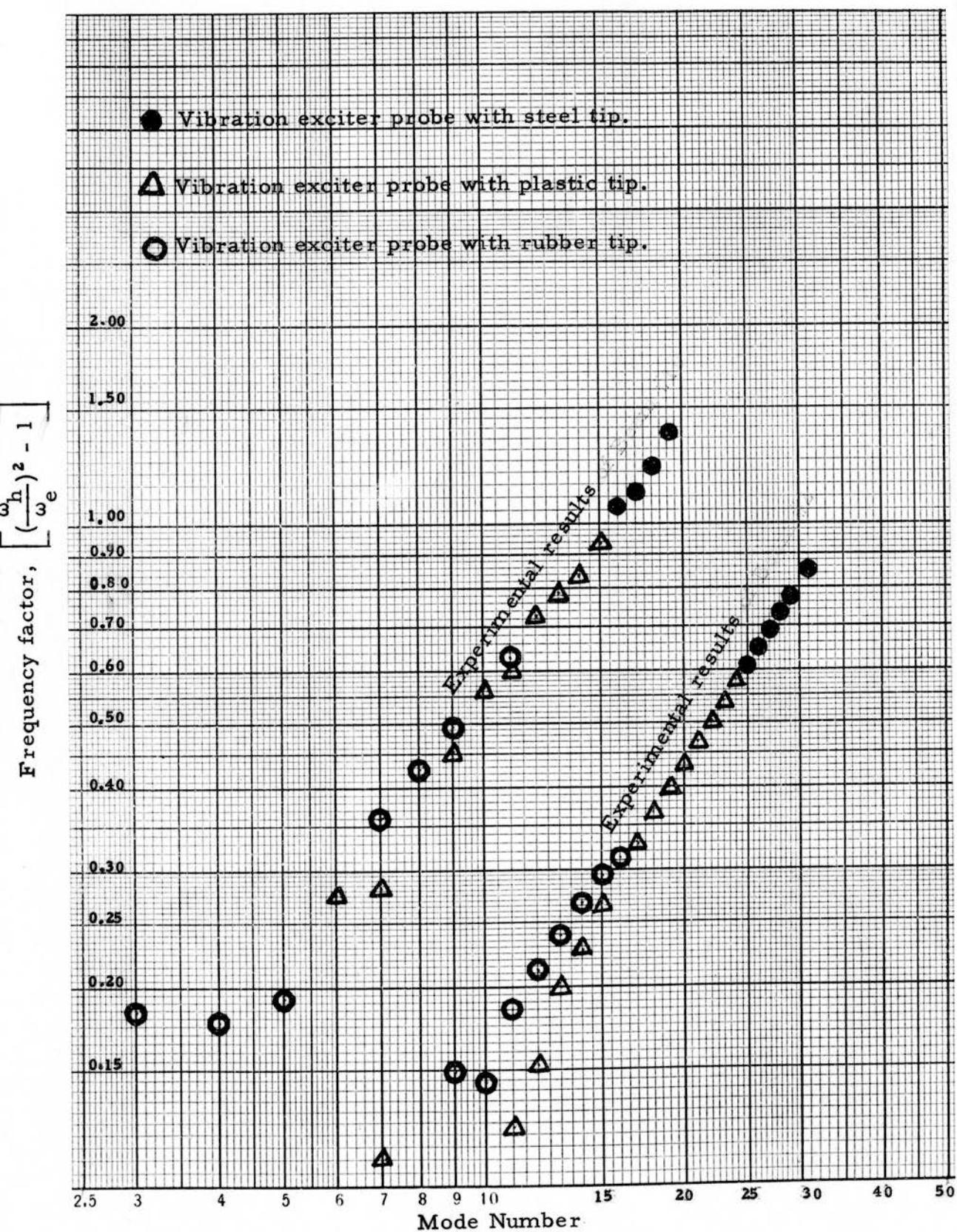


Fig. 5a. Experimental results of clamped beams Nos. 2 and 10.

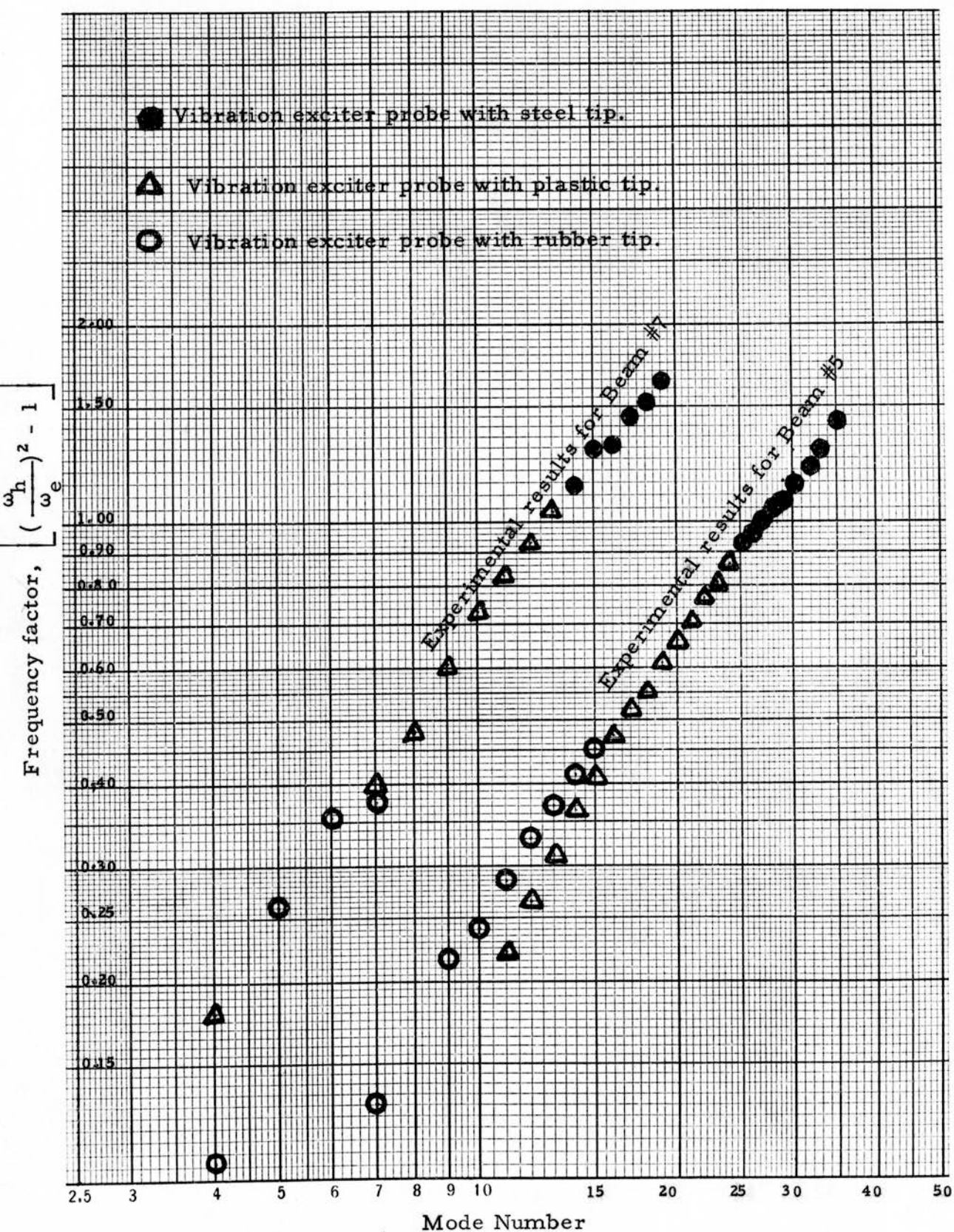


Fig. 5b. Experimental results of clamped beams Nos. 5 and 7.

the theoretical ones.

Sample Calculations

I. To find the natural frequencies of the simply supported, homogeneous beam.

The natural frequency is obtained from the equation:

$$\omega_h = \frac{m^2 \pi^2}{2 \pi} \sqrt{\frac{g E I_h}{\gamma l^4}} = c \sqrt{\frac{g E I_h}{\gamma l^4}} \quad (g)$$

where

$$c = \frac{m^2 \pi^2}{2} = \frac{\pi}{2}, \frac{4 \pi}{2}, \frac{9 \pi}{2}, \text{ etc.}$$

$g = 386$ in. per sec.,

$E I_h =$ Flexural stiffness in lb-in.²,

$\gamma =$ Beam weight in pounds per inch,

$l =$ Beam length in inches.

Considering beam No. 2 as a homogeneous beam, ω_h is determined by following substitutions in equation (g):

$E I_h = 36,475$ lb-in.² (determined experimentally),

$m = 15$, number of mode,

$\gamma = .02535$ lb per in.

$l = 120$ inches.

Therefore,

$$\omega_h = \frac{(15)^2 (\pi)^2}{2 \pi} \sqrt{\frac{(386)(36,475)}{(.02535)(120)^4}}$$

and

$$\omega_h = \underline{\underline{578.419}} \text{ c.p.s.}$$

II. To determine theoretical natural frequencies of simply supported sandwich beam.

From equation (a), for Beam No. 2,

$$\omega_m^2 = \frac{m^4 \pi^4 E}{l^4 (1 - \nu^2) \frac{\gamma}{6g}} \left(\frac{I_T}{1 + m^2 s} + I_F \right)$$

where $I_T = \frac{f f'}{f + f'} \left(c + \frac{f + f'}{2} \right)^2$ and $\rho = \frac{\gamma}{6g}$

For $f = f'$,

$$I_T = \frac{f}{2} (c + f)^2 = \frac{.016}{2} (0.25 + 0.016)^2 = \underline{\underline{5.6605 \times 10^{-4}}},$$

$$I_F = \frac{f^3 + f'^3}{12} = \frac{f^3}{6} = \left(\frac{0.016}{6} \right)^3 = \underline{\underline{0.682666 \times 10^{-6}}}$$

$$E = 10.3 \times 10^6 \text{ p.s.i.}; \quad \nu = 0.33$$

$$\gamma = 0.02535 \text{ lb per in.}; \quad l = 120 \text{ in.},$$

and $s = \frac{\pi^2 c f f'}{l^2 (f + f')} \frac{E}{G_{xz} (1 - \nu^2)} = \frac{\pi^2 c f}{2 l^2} \frac{E}{G_{xz} (1 - \nu^2)}$ where

G_{xz} is given by the manufacturer

$$= \frac{\pi^2 (0.25)(0.016)}{2 (120)^2} \frac{(10.3 \times 10^6)}{(11,700)(0.8911)} = \underline{\underline{1.35423 \times 10^{-3}}}.$$

On substitution of above values, and on further simplification

$$\omega_m^2 = \frac{(15)^4 \pi^4 (10.3 \times 10^6) (6) (386)}{(120)^4 (.8911) (0.02535)} \left[\frac{5.6605 \times 10^{-4}}{1 + (15)^2 (1.35 \times 10^{-3})} + .6821 \times 10^{-6} \right].$$

Therefore,

$$\omega_m = \underline{\underline{525.835 \text{ c.p.s.}}}$$

$$\text{III. } \left(\frac{\omega_h}{\omega_m} \right)^2 = \left(\frac{578.419}{521.835} \right)^2 = (1.1)^2 \\ = \underline{\underline{1.21}},$$

similarly,

$$\left(\frac{\omega_h}{\omega_e} \right)^2 = \left(\frac{578.419}{532} \right)^2 = (1.0873)^2 \\ = \underline{\underline{1.1821}}$$

IV. Per cent deviation of experimental values of natural frequencies from the theoretical ones.

$$\text{Per cent deviation} = \left(\frac{\omega_e - \omega_m}{\omega_e} \right) (100) \\ = \left(\frac{532 - 525.835}{532} \right) = \underline{\underline{1.158 \text{ per cent}}}$$

V. To find the value of s and G_{xz} for Beam No. 2.

Rewriting equation (f),

$$\log \left[\left(\frac{\omega_h}{\omega_e} \right)^2 - 1 \right] = 2 \log m + \log s. \quad (f)$$

For any mode number, say $m = 20$, it is seen from the curve for Beam No. 2 on Fig. 3a, that

$$\left[\left(\frac{\omega_h}{\omega_e} \right)^2 - 1 \right] = \underline{\underline{0.55}},$$

on substitution in (f)

$$\log (0.55) = 2 \log (20) + \log s,$$

$$\bar{1}.7404 = 2(1.3060) + \log s.$$

Therefore,

$$\log s = \bar{3}.1373 \text{ and } s = \underline{\underline{1.372 \times 10^{-3}}}$$

now, since $f = f'$

$$s = \frac{\pi^2 c f}{2 l^2} \frac{E}{G_{xz} (1 - \nu^2)},$$

therefore,

$$G_{xz} = \frac{\pi^2 c f}{2 l^2} \frac{E}{s (1 - \nu^2)}$$

$$= \frac{(\pi^2)(.25)(.016)}{2(14,400)} \frac{(10.3 \times 10^6)}{(1.372 \times 10^{-3})(.8911)}$$

$$= \underline{\underline{11,540}}$$

DISCUSSION OF TEST RESULTS

Graphical interpretation of the tests and calculated results are shown in Figs. 3 to 5 inclusive, for three different end conditions. Examination of the percentage deviation of the theoretical values from the observed values (in cols. 5 and 10 in table 1 (a,b), and Figs. 3(a,b), shows that the agreement between calculated and observed values is reasonable. A maximum deviation of 15 per cent was found at one calculated place; the majority of the results agreed within 10 per cent.

The deviation of the calculated results from observed ones can be explained if it is considered that the natural frequencies of given simply supported beams, of constant dimensions and physical properties depend on the value of the core parameter s , which in turn is a function of G_{xz} (modulus of rigidity in x-z plane). In other words, the accuracy of s depends upon the accuracy with which the value of G_{xz} is determined.

The determination of the value of G_{xz} required a relatively complicated test set-up, and in view of the lack of time to perform such a test, the values of G_{xz} which were reported by the manufacturer were used in calculating the natural frequencies at various modes. The theoretical curves in Figs. 3a and 3b were plotted from these values.

Therefore, no estimate of the accuracy of the values of s , and hence ω_m , can be given. However, the theoretical and experimental curves are both asymptotic to a straight line with a slope 2 and an intercept $\log s$. In view of this fact, straight lines are drawn through the plotted experimental results and the intercepts $\log s$, and hence the values of G_{xz} are

determined and listed in Table 4. These values are lower in case of strong core panels, and higher in weak core panels than the respective values reported by the manufacturer.

Smaller and larger values (because of different G_{xz}) of intercept log's, caused the shifting up and down of the theoretical curve of the weak and strong core beams, respectively. This implies that G_{xz} can be determined by vibration tests without destroying the panels, without having a complicated experimental set-up, and perhaps with better accuracy.

Further examination of the percentage deviations in Tables 1(a,b) shows that the deviations between the calculated and observed values are mostly greater in case of beams with a weak core than those in beams with a strong core. These discrepancies are also due to higher differences in the values (between those reported by manufacturer and those determined from vibration tests) of G_{xz} in case of weak core beams than those in strong core beams.

It is difficult to get beyond 35 modes in case of thin beams, partly because at higher modes the limiting factor is the force generating capacity of the vibration exciter, that is, the acceleration at such high frequencies is high, resulting in extremely small amplitudes to which the beam does not respond, and partly because of the fact that the Chladni pattern becomes smaller than the length between the other two free edges. Vibrations of this type are not accounted for by the theory.

Similarly, modes beyond 23 cannot be obtained for thick beams because their relatively higher stiffness requires higher frequencies for

resonance and the acceleration reached the maximum limit of the vibrator.

CONCLUSIONS

Conclusions derived from the limited number of tests performed are as follows:

The theory for natural frequencies of vibration of sandwich panels, simply supported on two opposite ends is verified.

The experiments indicate that theoretical formulas, similar to those of the Raville-Kimel theory for simply supported ends, exist for the free-free and clamped end sandwich panels.

Assuming that the theory is valid, the testing procedure can be used as a non-destructive method for the determination G_{xz} . When used this way, it yields values for G_{xz} which are consistent with those obtained by direct static methods.

ACKNOWLEDGMENTS

The author is highly grateful to Dr. Philip G. Kirmser and Dr. M. E. Rville for their encouragement, advice, and counsel during the course of the research work. He wishes to express his appreciation to Dr. W. R. Kimel and Dr. R. G. Nevins for their encouragement and kind help on many occasions.

Grateful acknowledgment is also due to Mr. Marion W. Davis, Department of Applied Mechanics, and Mr. Wallace Myer, a student colleague, for their valuable and sincere help with the equipment.

NOMENCLATURE

x, y, z	Rectangular co-ordinates (Fig. 1)
t	time co-ordinate
a	length of panel in direction of loading, (Fig. 1)
c	thickness of core, (Fig. 1)
f, f'	thickness of right and left facings, respectively, (Fig. 1)
E	Modulus of Elasticity of facings
ν	Poisson's ratio of facings
E_c	Modulus of Elasticity of core
G_{xz}	Modulus of Rigidity of core in xz plane
u_c, w_c	displacements of core in x and z directions, respectively
w	displacement in z direction of any point in sandwich
$\epsilon_{zc}, \gamma_{xzc}$	normal and shear strains, respectively in core
$\epsilon_{xM}, \epsilon'_{xM}$	membrane strains in right and left facings, respectively
$\epsilon_{xB}, \epsilon'_{xB}$	bending strains in right and left facings, respectively
σ_z, τ_{xz}	normal and shear stress, respectively, in core (Fig. 1)
V_c	elastic energy per unit width of core
V_{MF}, V'_{MF}	elastic energy per unit width associated with membrane strains in right and left facings, respectively
V_{BF}, V'_{BF}	elastic energy per unit width associated with bending strains in right and left facings, respectively
V	total elastic energy per unit width of panel
T	kinetic energy per unit width of panel

ρ	mass density of composite panel per unit length and width
δ	mass density of core per unit volume
ω_m	theoretical natural frequency of vibration of panel, radians per unit time
ω_e	experimental (observed) natural frequency of vibration of panel radians per unit time
ω_h	natural frequency of vibration of equivalent homogeneous beam, radians per unit time
m	integer
A_m, B_m, C_m, F_m	configuration parameters
I_F	$\frac{f^3 + (f')^3}{12}$
I_T	$\frac{f f'}{f + f'} \left(c + \frac{f + f'}{2} \right)^2$
γ	weight of the beam, pounds per inch
s	$\frac{\pi^2 c f f'}{a^2(f + f')} \quad \frac{E}{G_{xz}(1 - \nu^2)}$

REFERENCES

- (1) Kimel, W. R., and M. E. Raville
Natural frequencies of vibration of sandwich panels
hinged on two opposite edges.
Unpublished research paper, Kansas State College,
Manhattan, Kansas.
- (2) Timoshenko, S.
Vibration problems in engineering. New York:
D. Van Nostrand Co., Inc., 3rd ed., Jan. 1955.

APPENDICES

APPENDICES

To find the nodes and antinodes of a beam:

Let

$$X = c_1 \sin \beta x + c_2 \cos \beta x + c_3 \sin \beta x + c_4 \cosh \beta x \quad (1)$$

where $\beta = \sqrt[4]{\frac{\gamma \omega^2}{EIg}} \cdot ((2) \text{ p. 325})$

Equation (1) represents the deflection curve of a beam performing normal mode vibration.

The constants c_1 , c_2 , c_3 and c_4 can be determined from end conditions.

1. Beam with free-free ends:

On substitution of the end conditions, equation (1) reduces to the following:

$$X = \cosh \beta x - \sinh \beta x + \cos \beta x. \quad (2)$$

(a) At nodal positions, $X = 0$; therefore,

$$\cosh \beta x - \sinh \beta x - \sin \beta x + \cos \beta x = 0. \quad (3)$$

For even modes, the nodal position is always located at $x = 0.5$ for a beam of unit length, where x is the distance of the node from either of the ends.

For 6th mode,

Since, $\beta = 20.42033$ and $x = 0.5$ ((2) p. 336)

$$\beta x = 10.21016 \text{ radians.}$$

Therefore, $x = \frac{10.21016}{29.845} = \underline{\underline{0.342}}$

Table 5 presents the nodal positions for various modes.

(b) To find antinodal positions or positions of maximum amplitude for beams with free ends (for use in placing the vibration exciter).

Differentiate (2) with respect to x , gives

$$\frac{dX}{dx} = \beta (\sinh \beta x - \cosh \beta x - \sin \beta x - \cos \beta x). \quad (4)$$

At antinode, $\frac{dX}{dx} = 0$, therefore, (4) becomes

$$\sinh \beta x - \cosh \beta x - \sin \beta x - \cos \beta x = 0. \quad (5)$$

In the case of odd numbered modes, antinode always occurs at $x = 0.5$, therefore, for 9th mode, since $\beta = 29.845$ and $x = 0.5$ then $\beta x = 14.923$.

So, for 16th mode, since $\beta = 51.836$ and $\beta x = 14.923$ from which

$$x = \frac{14.923}{51.836} = \underline{\underline{.2885}}$$

2. Beam with clamped ends:

In this case, only antinodal positions are needed to place the vibration exciter and they are the same as free-free end beam.

3. Beam with simply supported ends:

In this case, also, only antinodal positions are needed to place the vibration exciter. On substituting the end conditions, equation (1) reduces to $X = D \sin \beta x$. (6)

Differentiating (6) gives

$$\frac{dX}{dx} = D \beta \cos \beta x. \quad (7)$$

For antinodal positions, therefore,

$$\cos \beta x = 0. \quad (8)$$

Since, the frequency equation in this case is

$$\sin \beta l = 0 \quad (9)$$

The values of β for unit length are

$$\pi, 2\pi, 3\pi, 4\pi, \text{ etc.}$$

The antinode always occurs at $x = 0.5$ for odd numbered nodes.

For 4th mode, since $\beta = 4\pi$ therefore $x = \frac{3}{8}$ to satisfy equation (8).

Table 5. Nodal and antinodal positions on the beam of unit length.

No. of modes	<u>For free-free ends beam</u>		<u>Clamped ends beam</u>	<u>Hinged ends beam</u>
	nodal posi- tion for strings	antinodal posi- tion for vibra- tion exciter	position for vibra- tion exciter	position for vibration exciter
1	0.244	0.5	0.5	0.5
2	.132	.308	.308	.25
3	.356	.5	.5	.5
4	.277	.389	.389	.375
5	.227	.5	.5	.5
6	.192	.423	.423	.5833
7	.3	.5	.5	.5
8	.265	.441	.441	.5625
9	.342	.5	.5	.5
10	.309	.454	.454	.45
11	.283	.5	.5	.5
12	.26	.321	.381	.5416
13	.315	.5	.5	.5
14	.293	.466	.466	.5357
15	.274	.5	.5	.5
16	.318	.41	.41	.5313
17	.30	.5	.5	.5
18	.284	.474	.474	.5278
19	.269	.5	.5	.5
20	.256	.428	.428	.525
21	.245	.5	.5	.5
22	.278	.433	.433	.5227
23	.266	.50	.50	.5
24	.245	.481	.481	.5218
25	.284	.5	.50	.5
26	.274	.444	.444	.5193
27	.264	.50	.50	.5
28	.255	.413	.413	.5179
29	.280	.50	.50	.5
30	.271	.484	.484	.5167
31	.262	.50	.50	.5
32	.254	.454	.454	.5156
33	.276	.500	.500	.5
34	.268	.428	.428	.5147
35	.260	.50	.50	.5

**NATURAL FREQUENCIES OF VIBRATION
OF SANDWICH PANELS**

by

MAGANBHAI PARBHUBHAI PATEL

B. Sc., University of Bombay, Bombay, India, 1949

B. S. University of Nebraska, 1952

B. S. University of Nebraska, 1953

**AN ABSTRACT OF
A THESIS**

submitted in partial fulfillment of the

requirements for the degree

MASTER OF SCIENCE

Department of Mechanical Engineering

**KANSAS STATE COLLEGE
OF AGRICULTURE AND APPLIED SCIENCE**

1959

Much work of both theoretical and experimental nature has been done in the field of statics of sandwich structures, but, to the knowledge of the author, very little work has been done previously in the dynamics field.

In view of these facts, Raville and Kimel presented a theoretical analysis for calculating the natural frequencies of vibration of sandwich panels, simply supported at the ends and constructed with isotropic facings and orthotropic cores.

This thesis presents an experimental verification of the theory and reports the development of vibration techniques for future investigations in this field.

Vibration tests were conducted for three end conditions,

1. Free-free,
2. Simply supported, and
3. Fixed-fixed.

In all cases the natural frequencies ω_m , derived from the Raville-Kimel theory where applicable, ω_h derived from the homogeneous beam theory, and ω_c , obtained experimentally, were determined. The Raville-Kimel theory predicts that certain functions of these quantities should be asymptotic to straight lines when plotted against the mode number on log-log paper. The slope of the straight line should be two, and the intercept determined by the value of G_{xz} , the shear modulus of the core.

The experimental data shows this character, and the value of G_{xz} obtained from the intercept method is approximately that obtained from

static tests as reported by the manufacturer of the sandwich material tested.

It is concluded that the Raville-Kimel theory is verified, and that it can be used in combination with the vibration tests described here as a non-destructive method for determination of G_{xz} .

Although there is no theory at present for the free-free and fixed-fixed end conditions, analysis of the data shows that theoretical results similar to that for the simply supported beams should exist.